

We are IntechOpen, the world's leading publisher of Open Access books Built by scientists, for scientists

6,900

Open access books available

185,000

International authors and editors

200M

Downloads

Our authors are among the

154

Countries delivered to

TOP 1%

most cited scientists

12.2%

Contributors from top 500 universities



WEB OF SCIENCE™

Selection of our books indexed in the Book Citation Index
in Web of Science™ Core Collection (BKCI)

Interested in publishing with us?
Contact book.department@intechopen.com

Numbers displayed above are based on latest data collected.
For more information visit www.intechopen.com



Perovskite Nanoparticles

*Burak Gultekin, Ali Kemal Havare, Shirin Siyahjani,
Halil Ibrahim Ciftci and Mustafa Can*

Abstract

2D perovskite nanoparticles have a great potential for using in optoelectronic devices such as Solar Cells and Light Emitting Diodes within their tuneable optic and structural properties. In this chapter, it is aimed to express “relation between chemical structures and photo-physical behaviours of perovskite nanoparticles and milestones for their electronic applications”. Initially, general synthesis methods of perovskite nanoparticles have been explained. Furthermore, advantages and disadvantages of the methods have been discussed. After the synthesis, formation of 2D perovskite crystal and effects on shape factor, particle size and uniformity of perovskite have been explained in detail. Beside these, optic properties of luminescent perovskite nanoparticles have been summarized along with spectral band tuning via size and composition changes. In addition, since their different optical properties and relatively more stable chemical structure under ambient conditions, a comprehensive compilation of opto-electronic applications of 2D perovskite nanoparticles have been prepared.

Keywords: perovskite, nanoparticle, nanocrystal, opto-electronics, solar cells, OLEDs, fluorescence

1. Introduction

Inorganic and/or hybrid perovskites have become prominent in solution-processed optoelectronics. Thousands of reports have been proposed about photovoltaics [1–3], light-emitting diodes (LEDs) [4–6], lasers [6, 7] and photodetectors [8–12] containing perovskite semiconductors per annum over the past decade. Halide perovskite nanostructures exhibit tremendous optic and electrical properties such as strong absorption and/or emission, higher photoluminescence quantum yields (PLQYs) [13–15], higher exciton binding energies and tuneable bandgaps than those of bulk perovskites and other nanomaterials. With these outstanding properties, they may offer many scopes for optoelectronics. Particularly, hybrid lead halide perovskite nanostructures (PNSs) offer unique opportunities for light-emitting diode (LED) applications. PNSs represent larger exciton binding energies and longer carrier decay times than those of bulk crystals. In addition to this, their narrow emission band makes them good candidates for LED [16] and laser [17]. Since Schmidt et al. reported the synthesis of first colloidal PNS by a simple procedure under ambient conditions in 2014 [18], many research groups have started working on these materials. In the synthesis of PNSs, it is possible to use organic ligands for capping to stop crystals' growth in the nanometer scale. Furthermore,

capping ligands can reduce surface defects in the same way of the traditional NC preparation. Thus, size and shape of PNSs can be tune finely from a single perovskite layer or below the exciton Bohr radius for using the effect to quantum confinement to multilayers which exhibits bulk-like properties. With this method, it is possible to prepare nanostructures like quantum dots (QDs), nanoplatelets (NPLs), nanosheets (NSs), and nanowires (NWs) [19, 20].

In a simple PNS growth process, the methylammonium cations are embedded in the voids of the corner-sharing PbX₆ octahedra, the long alkyl chain cations only at the periphery of the octahedra with their chains hanging it. Therefore, long alkyl-ammonium ions can be used as the capping agents to limit the growth of the PNSs in three-dimension (3D). There are five common methods proposed in the literature which exhibits good prospects for obtaining various uniform and defect free PNSs. These are named as solvent-induced precipitation, hot injection, template assisted, ligand assisted reprecipitation and emulsion methods [13, 14].

In order to determine the structural and optic properties of PNSs, some characterization techniques such as small angle x-ray scattering (SAXS), scanning electron microscope (SEM), absorption and emission spectroscopy have been used extensively. It is crucial to know the shape and optical response of the nanocrystals for the further opto-electronic application of them.

As it is mentioned above, well-defined PNSs were used in many applications such as optical lasing and LEDs. Some of those applications have been investigated intensively by many groups all around the world. Some milestone studies have been presented comparatively.

2. Synthesis of nano-crystalline perovskites

There are many proposed methods for synthesis of PNSs by many groups in the literatures. Here we would like to express five of most common and essential methods (**Figure 1**) [21–23].

2.1 Solvent-induced precipitation

The physical properties of perovskite cluster such as size of NPs can be arranged by using long alkyl chain amine derivatives while oleic acid ensures the colloid stability via preventing the aggregation. In order to initiate the solvent-induced precipitation, and obtain colloidal MAPbBr₃ NPs, lead bromide (PbBr₂) and methyl ammonium bromide (CH₃NH₃Br) were mixed with Octylammoniumbromide (OABr) in acetone with oleic acid (OAc) and octylamine and the solution were kept at 80°C. The PLQY of obtained NPSs was about 20% as well as stable over three months. After this first attempt, PLQY of NPSs was increased up to 83% by optimization of the molar ratios of starting materials [22, 24].

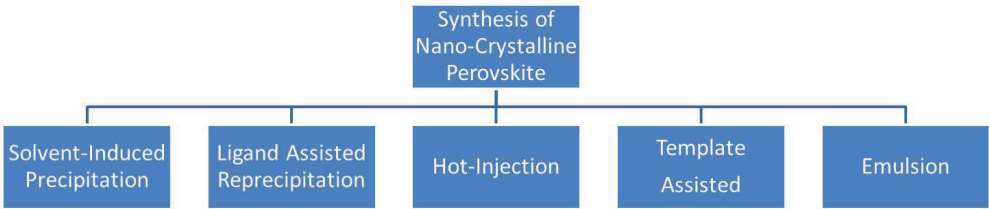


Figure 1.
Common synthesis methods for perovskite nano-crystals.

2.2 Ligand assisted reprecipitation (LARP) technique

In this method, a polar solvent such as dimethylformamide (DMF) which dissolve all starting materials and capping ligands have been used to prepare the precursor solution [25, 26]. This solution is added dropwise into vigorously stirred toluene which is not a good solvent for starting materials and perovskite crystal. Zhang et al. has demonstrated the synthesis of colour- tuneable PNSs (average particle size of 3.3 ± 0.7 nm) with a PLQYs of 50–70% (**Figure 2**) [25]. It was claimed that a slight descending of PLQY was observed by the ascending of the size of the perovskite crystal ($2\text{--}8\text{ }\mu\text{m}$, PLQY $< 0.1\%$). In the nanometer scales, surface defects of the crystals can easily be passivated by ligands. Thus, most of the photo-generated charges can recombine before there are trapped by defects on the surface. However, due to the less ligand passivation, the number of defects on the bulk perovskite structure's surface, which increased the number of trapped charges, are significantly high, resulting very low PLQY. In another study, well-defined cubic and thermally stable FAPbX_3 nanocrystals (about 10 nm) has been prepared by LARP method. The reported PLQY for the NPS was 75% [27]. A new procedure, which was used to obtain a core-shell shape by using the LARP approach has been recently demonstrated. With this proposed method, a solution-processed, stable core-shell-type Methyl ammonium (MA^+) + Octyl ammonium (OA^+) lead bromide perovskite NPs ($\approx 5\text{--}12$ nm) with good PLQY was prepared. In addition to this, Core-shell-type NPs was accomplished by systematically changing the molar ratio of capping ligands, OABr, and MABr without altering total amount of alkylammonium bromide and synthesis conditions. The color tunability of NPs in the blue to green spectral region (438–521 nm), high PLQY, and reasonable stability under ambient condition are credited to the quantum confinement imparted by the crystal engineering associated with core-shell NP formation [28–30].

2.3 Hot injection method

The stability of inorganic perovskites is significantly higher than that of hybrid perovskite crystals. By changing the organic cation with an inorganic one (e.g., Cs),

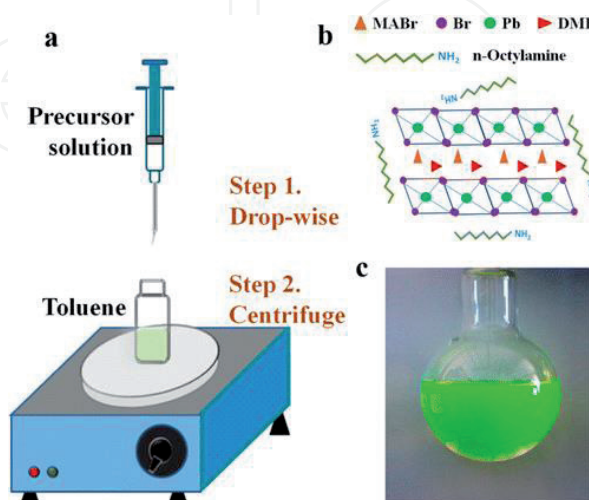


Figure 2.
(a) Schematic illustration of Set up for LARP; (b) starting materials and shape of perovskite nano-crystals; (c) image of typical solution containing $\text{CH}_3\text{NH}_3\text{PbBr}_3$ nano-structures (reproduced with permission of Ref. [26]).

chemical and thermal stability of Perovskite material can be increased greatly (Figure 3) [31, 32]. It is possible to obtain various crystal phases by changing the temperature resulting a shifting in the optical responses. The hot injection method is a widespread method for synthesizing inorganic PNSs. In a typical synthesis procedure, a solution of PbX_2 ($\text{X} = \text{I}/\text{Br}/\text{Cl}$), in octadecene (ODE) along with oleic acid and oleyl amine is prepared. During stirring, Cs-oleate is injected into that solution quickly under dry condition at $140\text{--}200^\circ\text{C}$ [32]. To quench the reaction (after 5–10 sec), the reactor is cooled with an ice bath. With this method, it is easy to obtain uniform nano-cubes with the size of 4–15 nm edge length representing high PLQY, up to 50–90% and a very narrow emission band (12–42 nm) in the visible region (410–700 nm). As it was mentioned before, the optical properties of the NPSs are related to shape, size,

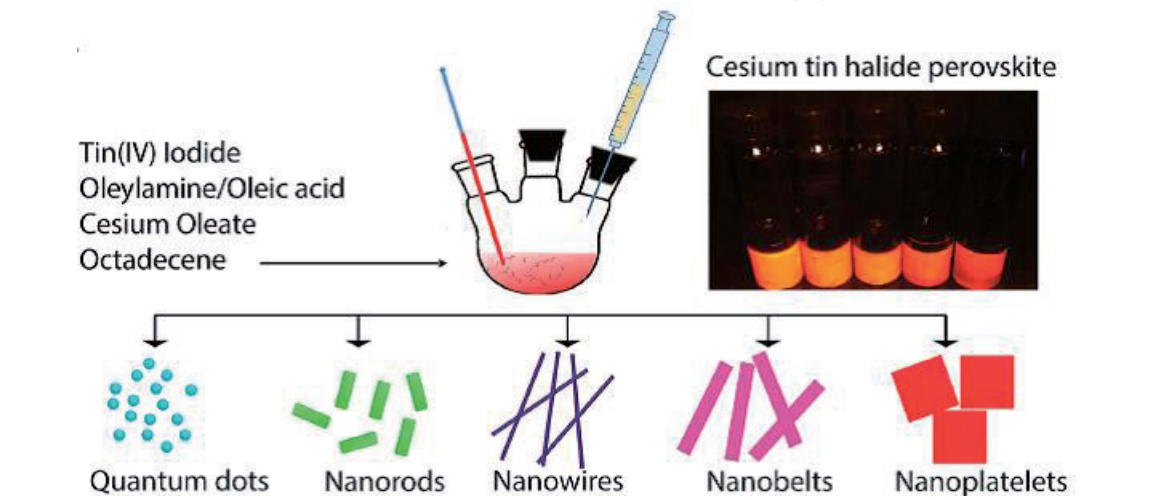


Figure 3. Schematic illustration of Hot-injection method (left-hand), image of Cs_2SnI_6 samples under UV-light (right-hand) and possible crystal shapes obtained by hot-injection method (reproduced with permission of Ref. [33]).

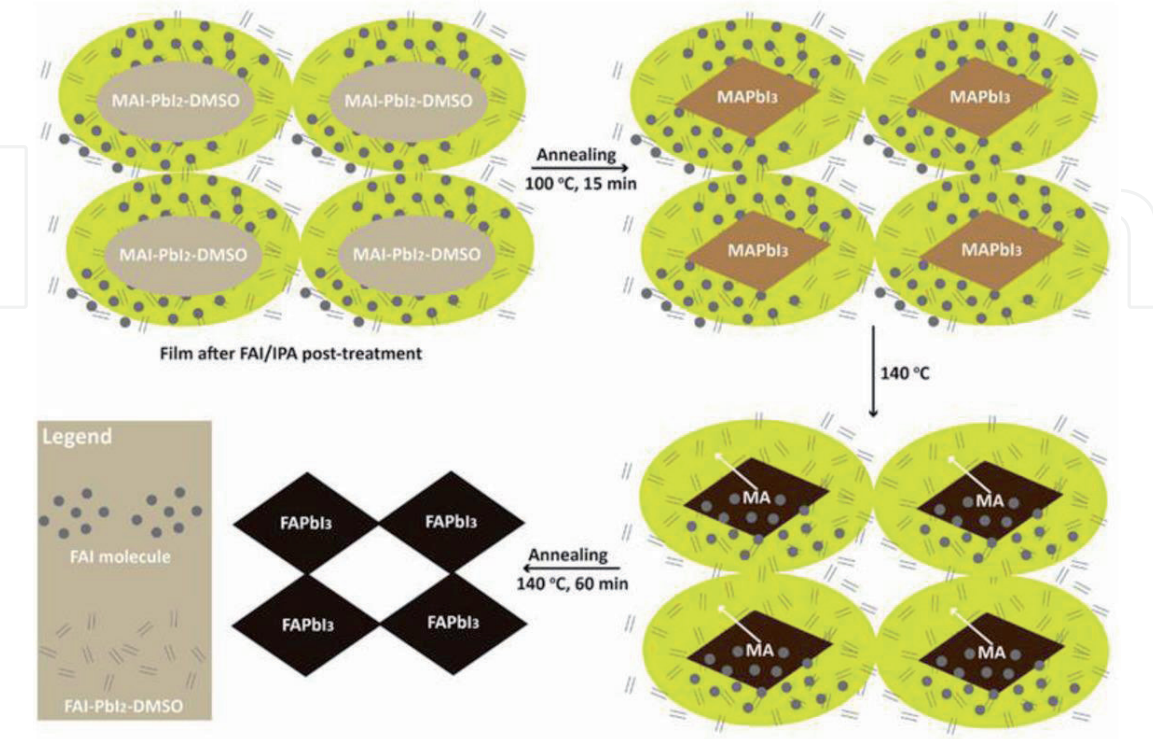


Figure 4. Schematic illustration of perovskite nano-crystal preparation by the template-assisted method (reproduced with permission of Ref. [36]).

and surface chemistry of them due to the significant changes in the band structures. Therefore, by the variation of the surfactants, ligands, reaction temperature and time, the perovskite precursor composition can be adjust [33] to realize the formation of nanowires, nanoplatelets, spherical dots, and nanorods (**Figure 3**) [33–35]. A critical point for the hot injection is the reaction temperature effecting the size of the NPSs. To overcome this disadvantage, new methods have been developed for hybrid perovskites.

2.4 Template-assisted method

In this synthesis approach, NP formation is induced by a specific substrate such as mesoporous silica and aluminum oxide film as a template [36–38]. NPSs is obtained on the films which exhibits intensive light. This technique is suitable for formation of mono disperse NPSs with various narrow emissions (full width of half maximum (FWHM) is less than 40 nm) bands from green (FWHM: 22 nm) to near infrared (FWHM: 36 nm) by template optimization [37–39]. In a recent study, perovskite nanocrystals have been prepared in a nano-porous structure. By this kind of strategies, it is possible to confine PNSs (<10 nm) without any capping agents (**Figure 4**). In other words, the emission wavelength of perovskite nanoparticles can be arranged precisely for sophisticated photonic applications such as lasers [36, 37].

2.5 Emulsion method

In order to control the crystallization of perovskite and obtain uniform NPs, emulsion synthesis method was modified [40]. By using this method, it is possible to tune the size of PNSs under 10 nm with an PLQY up to 92% [41]. In this method, an emulsion is prepared with two immiscible solvents. After that, a demulsifier is added into this for initiating solvent mixing and start crystallization (**Figure 5**). For this procedure, DMF and n-hexane are very good candidates as immiscible solvents while tert-butanol or acetone is used as demulsifier solvent [41]. This method is suitable to obtain PNSs in solid state which can be used in another solvent matrix for an application later. Furthermore, long alkyl ammonium halides are used as capping agent.

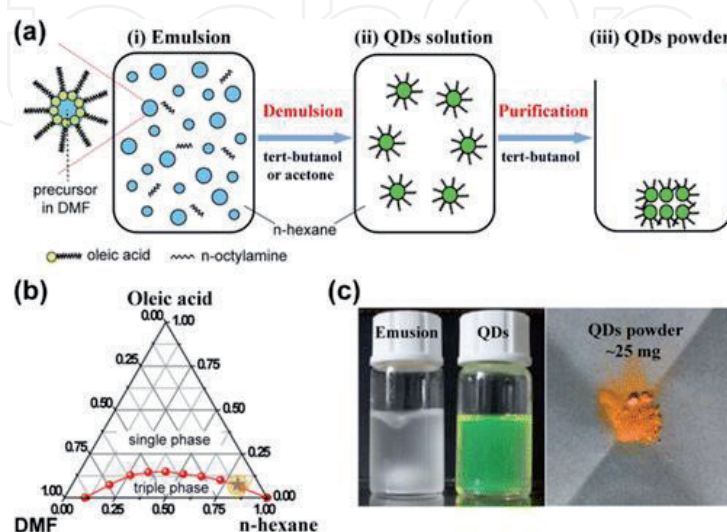


Figure 5. (a) Schematic illustration of preparation of nano-crystals by emulsion method; (b) ternary phase diagram (DMF/OA/n-hexane); (c) image of a typical $\text{CH}_3\text{NH}_3\text{PbBr}_3$ emulsion, colloidal NP solution and solid-state powder of $\text{CH}_3\text{NH}_3\text{PbBr}_3$ NPs (reproduced with permission of Ref. [41]).

3. Form factor of perovskite nano-crystals

3.1 Crystal shape of perovskite nano structures

As it is well known, semiconductor perovskite crystalline structure has a general formula of ABX_3 where A is an organic or inorganic cation, organic methylammonium (MA^+), formamidinium (FA^+) or inorganic cesium (Cs^+); B is a metal cation typically lead (Pb^{2+}) or tin cations (Sn^{2+}); and X is a halide anion. Cation A is slightly larger than centred cation B having 6 co-ordination number. There is a significant relationship, which is called “Goldschmidt Tolerance Factor” between the size of the ions and the formation and the shape of the crystal structure:

$$t' = \frac{r_A + r_X}{\sqrt{2}(r_B + r_X)} \quad (1)$$

Where, r_A and r_B are cationic diameters of A and B respectively, and r_X is the anionic diameter of halide in Å. When cation A is too big or cation B is too small (>1), hexagonal perovskite crystal is formed. If cation A and has the ideal size ($0.9 < t < 1$), cubic perovskite crystal is formed. Finally, if cation is too small to fit into the space between metal cations (B) ($0.7 < t < 0.9$), orthorhombic perovskite structure is formed [42].

3.2 Geometry of perovskite nano-crystals

A typical “bulk” perovskite structure is called three-dimensional (3D) which is usually comply to the ABX_3 formula completely [43–45]. In this situation, “3D” refers to the growth in every dimension without any confinement. X anions are combined through corner sharing to form a 3D network. Beside this, the cation A occupies the site in the middle of eight octahedra, and each element needs to owe the proper valence state to keep a whole charge balance [43]. To obtain nano crystal-line perovskites, crystal growth must be restricted with at least one dimension by a capping agent or a matrix. Thus, It is possible to prepare various dimensioned PNSs such as zero, one or two dimension (0D, 1D or 2D respectively) (**Figure 6**) [1, 46].

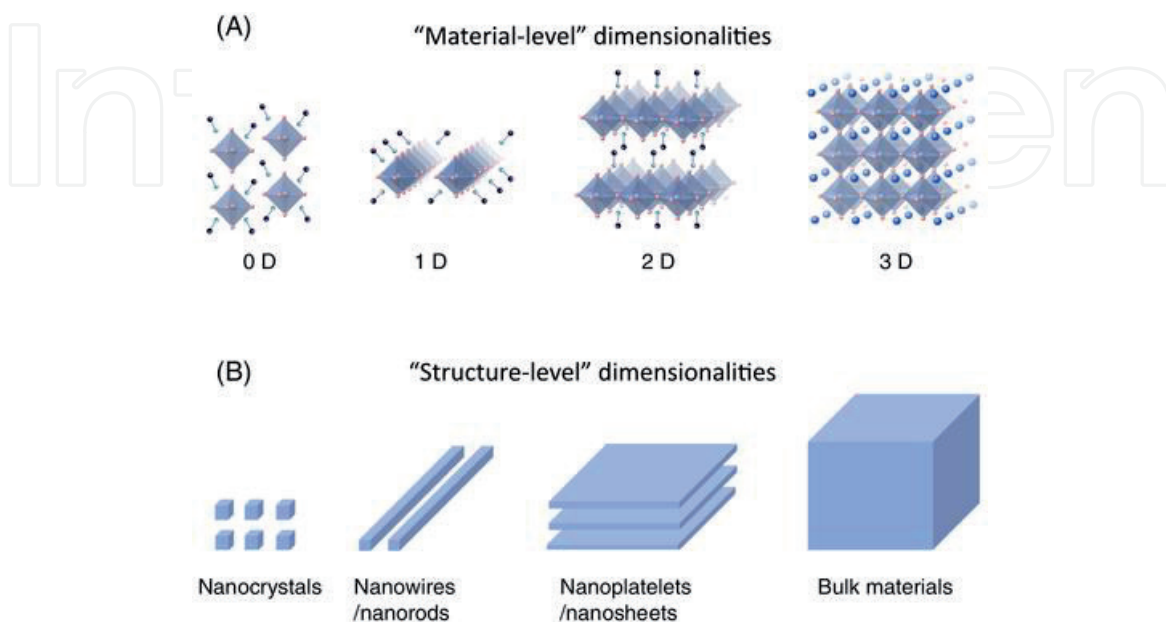


Figure 6. Schematic illustration of low-dimensional perovskites and 3D perovskite crystal structures (reproduced with permission of Ref. [47]).

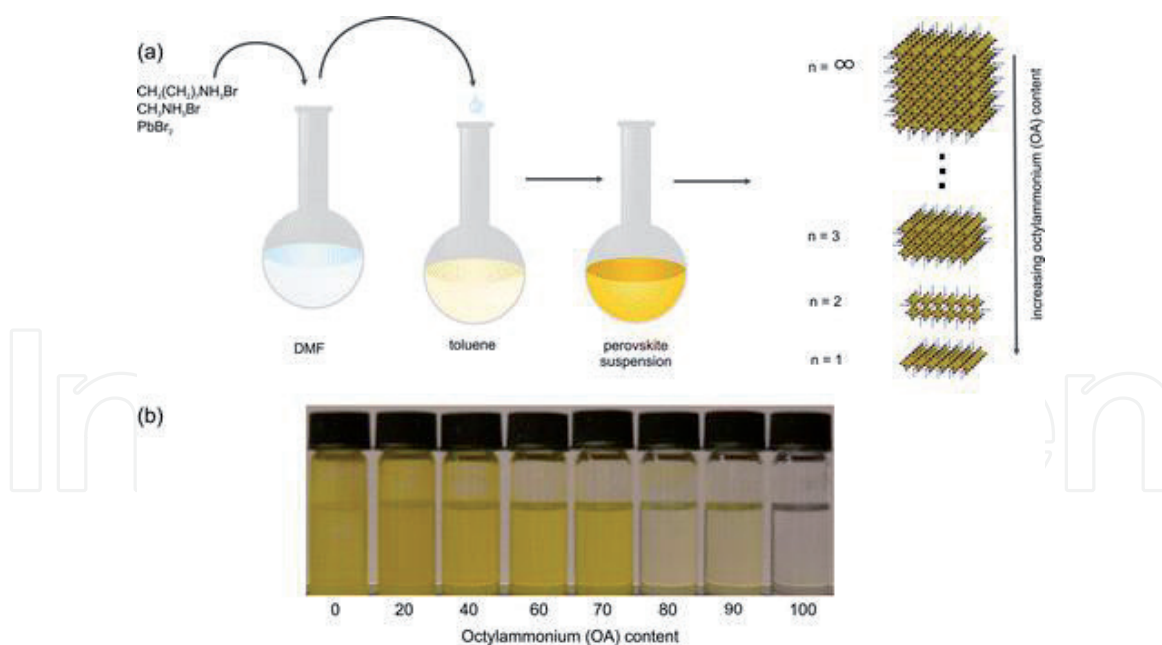


Figure 7.
(a) Schematic illustration of the perovskite nanoplatelets preparation. (b) Image of OA/MA perovskite suspensions in toluene under ambient light (reproduced with permission of Ref. [49]).

0D PNSs have been synthesized, by LARP [25], hot-injection [32] and template-assisted method [36] by different groups. Crystal growth is prevented in all dimensions by a ligand or a metal-oxide matrix to obtain quantum-dot-like NPs representing good Photoluminescence (PL). Prepared nanostructures have been used in many opto-electronic applications such as solar cells, LEDs and laser.

Perovskite nanowires or nanorods are basically 1D PNSs which represent outstanding anisotropic optical and electrochemical properties with very high PLQFs [41]. 1D PNSs have been proposed by Horvath et al. for the first time in the literature. Nanowires with 50–400 nm wide and 10 μm length has been prepared in DMF solution phase. Obtained NPs have been used in Solar Cells [48], LED [4] and photodetector [8] applications.

Consequently, 2D PNSs are nano pellet or nano sheet shaped materials which consist of several unit cells leading larger binding energy for the exciton and more intense PL. These types of NPs have similar networks with corresponded 3D perovskite, however the general formula of ABX_3 is changed when the NP is very thin. Number of sheets in a nano pellet NPS can be determine by using absorption and emission spectroscopy. Differences of Absorption and emission maximum of nanosheets ($n = 1, 2, 3$ and 4) are very significant. Maximum absorption peak is red shifted with the increasing of number of unit cell (nano- pellet) (**Figure 7**).

4. Applications of perovskite nanoparticles

4.1 Optical properties of perovskite nanoparticles

In recent years, perovskite is a very important milestone in solar cell research, thanks to its perfect exciton and charge carrier properties. This excellent performance has allowed perovskite to be used as outstanding light emitters in Light Emitting Diodes (LEDs) and other optoelectronic applications [4, 7, 25, 50–56]. One of the most attractive features of perovskites is their emissions, which can be easily adjusted in the visible range compared to traditional III–V and II–VI groups. All inorganic-perovskite ABX_3 emissions, including quantum dots and nanoplatelets,

can cover the entire visible area, even close to the infrared or ultraviolet region, by substituting halide elements from chloride to iodine [26, 34, 51, 57, 58]. Another way to adjust the emission is to insert other organic molecules into it or replace anions/cations.

4.2 High quantum efficiency

Perovskites are considered superior light emitters owing to their large absorption coefficients and high quantum yields [59, 60]. The high quantum yield generally indicates that most of the absorbed photons are transformed by radiative recombination processes. High quantum yields (90%) have been reported in inorganic ABX_3 and organic-inorganic methyl-ammonium halide perovskite nanocrystals without further surface treatment [26, 34]. However, the main reason for reduced quantum efficiency in conventional III–V and II–VI groups is that these nanocrystalline structures are often affected by surface defects or donor-receptor levels. In perovskite, where there are very few electrical charge trapping conditions, high quantum efficiency is the result of the formation of a clear band gap that greatly supports exciton radial recombination efficiency [61].

4.3 Quantum confinement effect

Optical absorption and emission characteristics of a semiconductor can be adjusted by changing the size of the semiconductor. If the size of such materials is in the nanocrystal range, changes in band gaps can be observed. The reduction of the crystal size causes the quantum capture effect to be observed and the bandwidth to shift to blue. If the semiconductor size is too small to compare with the Bohr radius of excitons, quantum trapping can be seen in the optical properties of the semiconductors. For example, the quantum capture effect is quite evident in completely inorganic $CsPbBr_3$ perovskite nanocrystals and in organic-inorganic methyl ammonium lead halide perovskite nanocrystals. This can usually be observed when the nanocrystalline size is comparable to the exciton Bohr radius. **Figure 8a and b** demonstrate that the emission of $CsPbBr_3$ perovskite nanocrystals can actually be adjusted from 2.7 eV to 2.4 eV, with a size ranging from 4 nm to 12 nm, which is compatible with the theoretical calculation [34].

4.4 Linear absorption and emission

Many groups have focused on improving the band spacing, excitonic characteristic and optical properties of photoluminescent quantum yields of halide perovskite nanocrystals for optoelectronic applications in recent years [18, 62]. The most interesting of these features is that bandwidth is adjustable. It is possible to adjust the bandwidth by changing the individual components of the metal halide perovskites (MHP). Optical properties of bulk perovskite thin films could be changed across the entire visible spectrum. Thus, it has been shown that the optical properties of $MAPbBr_3$ nanocrystals, which have an emission of approximately 529 nm, can also be altered throughout the entire visible spectrum [63, 64]. For $CsPb(X = Cl, Br \text{ or } I)_3$ nanocrystals, using halide components, the emission wavelength is from 410 nm ($X = Cl$), ($X = Br$) to 512 nm, ($X = I$) It has been shown that it can be shifted to 685 nm (**Figure 9**).

Adjustable optical features of perovskite nanocrystals are based on the electronic structure of these materials (**Figure 10**). The conduction band consists of external p orbitals of halid and antibonding orbitals of hybridization of Pb 6p orbitals. The valence band consists of antibonding of the hybridization of Pb 6s

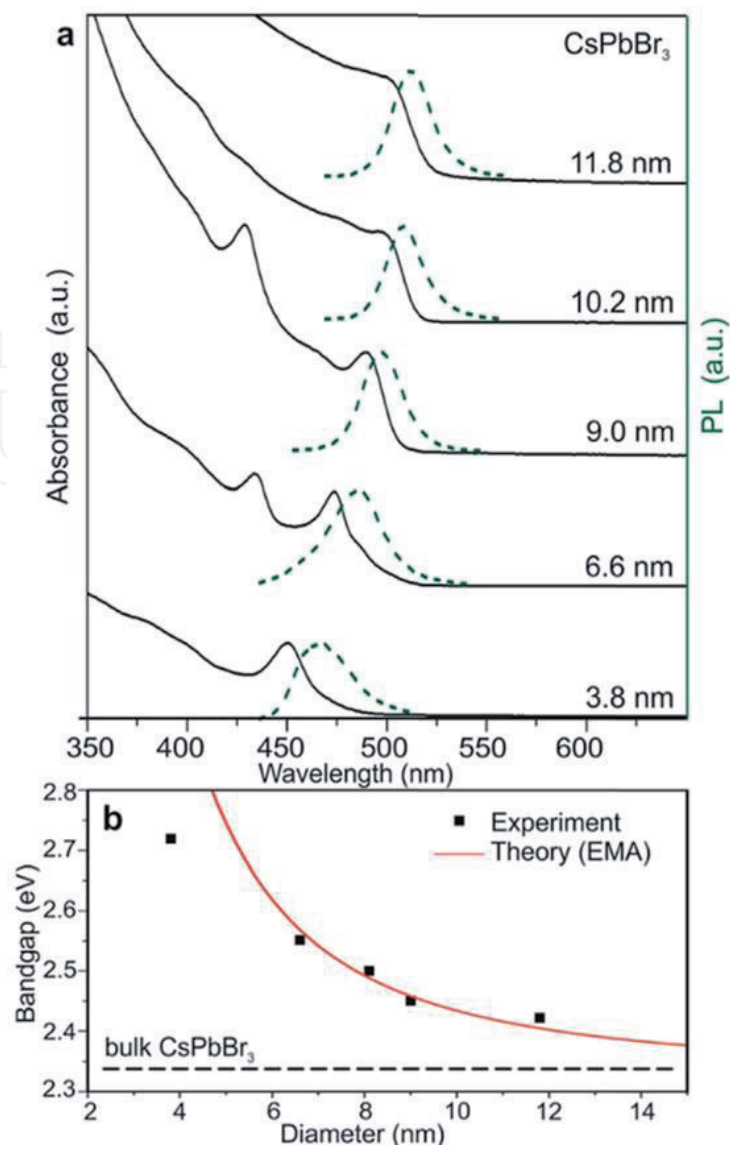


Figure 8.
(a) The emission spectra of CsPbBr₃ NCs Quantum-size effects in the absorption and (b) experimental versus effective mass approximation size (theoretical technique) with respect to the band gap energy range (reproduced with permission of Ref. [34]).

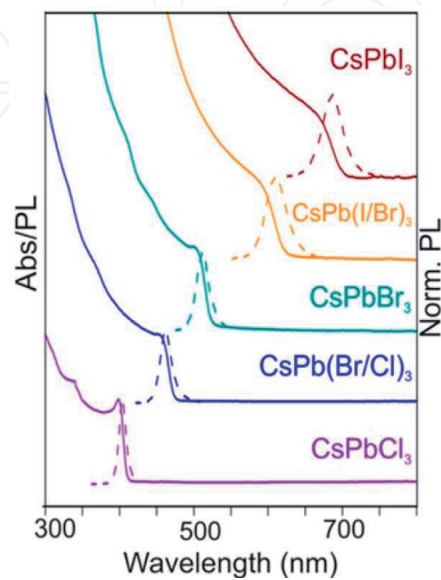


Figure 9.
UV-vis and photoluminescence spectra shows that the band gap could be tuned by controlling of CsPbX₃ NCs as a function of halide (reproduced with permission of Ref. [34]).

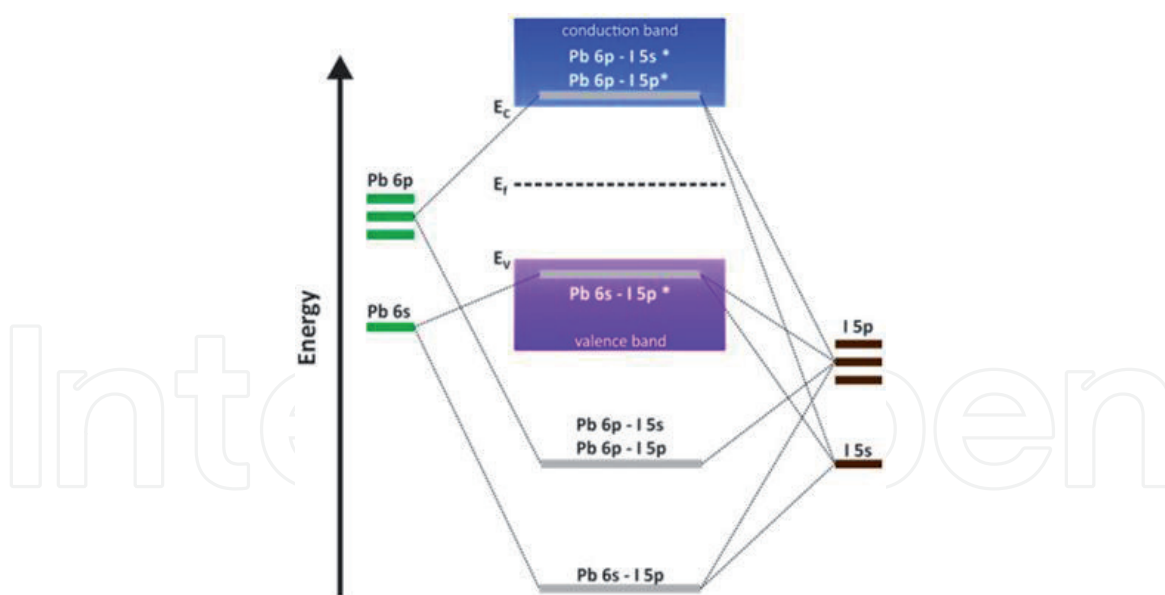


Figure 10.

The energy bands forms in a lead iodide perovskite by the crossing of lead and iodide orbitals (reproduced with permission of Ref. [23]).

and the same halide p-orbitals. The conduction band is generally p-like owing to the high density energy bands lead density contribution [65]. However, as the opposite of this situation, the band gap of gallium arsenide occurs between bonding and antibonding orbitals. As the halide component changes, the valence energy band shifts at the limit value, while only small changes occur in the energy limit value of the transmission band [66]. The cation A does not contribute considerably to the conduction and valence orbitals, but has an important effect on the band gap of perovskite [67]. As a result, emission energies of MA-based perovskite nanocrystals have been demonstrated to range from halide to 407 to 734 nm. It is understood that the FA emissions of nanocrystalline FAs shifted to 408 nm with Cl, to 535 nm with Br and to I and 784 nm, that is, to red [68–70]. In addition, the B cation has a significant mission in changing the optical properties of metal halide perovskites nanocrystals. As is known, the lead is a harmful element for the nature, instead of using the band [71], the band gap and PL emissions of the metal halide perovskites nanocrystals shifted from Cl to 443 nm and from I to 953 nm. The reason is probably a result of the higher electronegativity of Sn^{2+} than Pb_2 [72]. But, the stability of Sn^{2+} and similarly Ge^{2+} based on perovskite compounds is too weak owing to the reduction of non-interacting electron pair effects corresponding to a decrease in the stability of the divalent oxidation state [73]. As a result, PL emissions or energy band gaps of nanocrystalline structures obtained by various methods depend only on stoichiometry [74]. Stokes shift is an important parameter at the absorption and emission spectra that LHP nanocrystals show typically small, ranging from 20 to 85 meV [75–77]. Stokes shift increases as nanocrystals decrease in size. This is clarified by the creation of a compatible hole state that can be delocalized across the whole nanocrystal [78]. PL line widths of metal halide perovskites are another important point, particularly for LED applications. In fact, the line widths are commonly in the range of 70–110 meV and have been found to vary significantly with respect to the halide content. In many articles, the halide component greatly varies the PL spectra in terms of wavelength, for instance for Cl-perovskites reaches to 10–12 nm and for I-perovskites 40 nm. In terms of photoluminescent quantum yields, LHP nanocrystals display high values with the more epitaxial shell range the more chalcogenide QDs without electronic passivation [69]. Some article abot MA based halide perovskites have been reached to 80 % to 95 % for photoluminescent

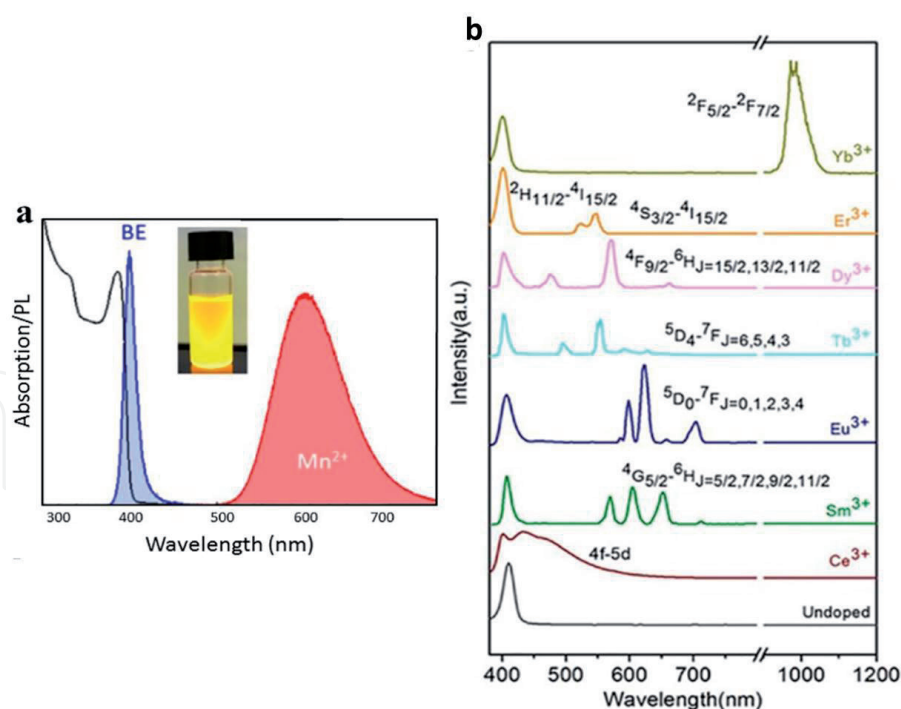


Figure 11.
(a) Photoluminescence emission & absorption of Mn-doped CsPbCl₃ NCs, (b) photoluminescence curves of CsPbCl₃ NCs doped with different lanthanide ions (reproduced with permission of Refs. [23, 87]).

quantum yields, bromide and iodides, respectively [79–82]. The defect tolerance of halide perovskite gives new properties due to orbital structure and the bandgap that forms between two antibonding orbitals. FA-based nanocrystals also reach to 70–90% photoluminescent quantum yield. There is alternative method that doping with additional ions to handle the optical emission of LHP nanocrystals. The addition of Mn²⁺ ions leads to a strong Stokes shift emission by the band gap given by the perovskite matrix and the emission from the atomic states of the Mn²⁺ ions (**Figure 11a**) [83]. Mn²⁺ doping can result in a pair of controllable emissions from both localized Mn²⁺ states and band gap recombination [84, 85]. In contrary, CsPbBr₃ nanocrystals have been shown to cause blue shift of doping, band boundary and PL emission with other divalent cations such as Sn²⁺, Cd²⁺ and Zn²⁺. In these cases, an important portion (0.2–0.7%) of the original Pb ions have been exchanged by new metal cations that produce alloy nanocrystals. CsPbBr₃ alloy nanocrystals with 0.2% content of Al³⁺ ions have a blue shear PL emission with a centre of 456 nm and a relatively high 42% photoluminescence quantum yield [86]. In all these cases, perovskite nanocrystals act as an absorbent host that stimulates dopants through energy transfer. In addition, by selecting specific dopant atoms, the emission wavelengths of the nanocrystals obtained can be easily adjusted. When lanthanide ions are doped, the emission of CsPbCl₃ nanocubes ranges from 400 nm to 1000 nm and their quantum yields are 15% and 35%, respectively (**Figure 11b**) [87].

5. Optoelectronics applications of perovskite

5.1 Optical lasing

High absorption coefficient and strong photoluminescence is the most powerful side of metal halide perovskite. It is possible to obtain a laser with a high quantum efficiency material and a suitable optical band spacing. With the understanding

that amplified spontaneous emission can be obtained from perovskite material, research has focused on this subject. Especially, laser obtaining studies were carried out by using perovskite crystal. It has also been shown that perovskite nanowires in high crystalline feature can have a Fabry-Perot gap to obtain a laser in the material [88]. By manipulating the content of the halide in the composition of the perovskite lead to control the emission wavelength and obtain the laser in the entire visible spectrum (**Figure 12a** and **b**) [57]. Zhu et al. showed that laser exposure in $\text{CH}_3\text{NH}_3\text{PbX}_3$ with an exponentially low current threshold (220 nJ cm^{-2}) and a corresponding carrier density as low as $1.5 \times 10^{16} \text{ cm}^{-3}$.

5.2 Light emitting diodes

Metal halide perovskite has great potential due to its easy preparation, low cost and high-performance light emitting diodes. Perovskites in LED applications show well a high colour purity, usually 15–25 nm full width half-colour purity for electroluminescence spectra. The point is here that the colour adjustment can cover the entire visible part of the spectrum by changing the content of different halides within the compounds. Therefore, many researchers have achieved high performance in perovskite quantum dot LED because of their quantum dots, strong luminescence, and high external quantum yields (**Figure 13a**) [25]. The stability problem of organic-inorganic hybrid perovskite can be eliminated by synthesizing the inorganic perovskites (ie CsPbX_3) as quantum dots for LED applications (**Figure 13b**) [89]. The performance of perovskite nanoplatelets in LED applications was lower than the quantum dots (**Figure 13c**). As a result, perovskite has a great potential for lighting and display applications as a new generation LED material.

5.3 Alternative applications

FETs, photodetectors, and single photon emitters are the other potential optoelectronic application devices. Liu et al. [90] used perovskite nanoplatelets to produce a FET on a Si/SiO_2 . For this device, the current-voltage curve showed ohmic contact between the perovskite nanoplatelets and electrodes, and a linear dependency was noted. In that study, they revealed a strong light-material interaction and broadband light harvesting capability of perovskite. Many photodetectors were fabricated based on a horizontal $\text{CH}_3\text{NH}_3\text{PbI}_3$ nanowire array [49]. The

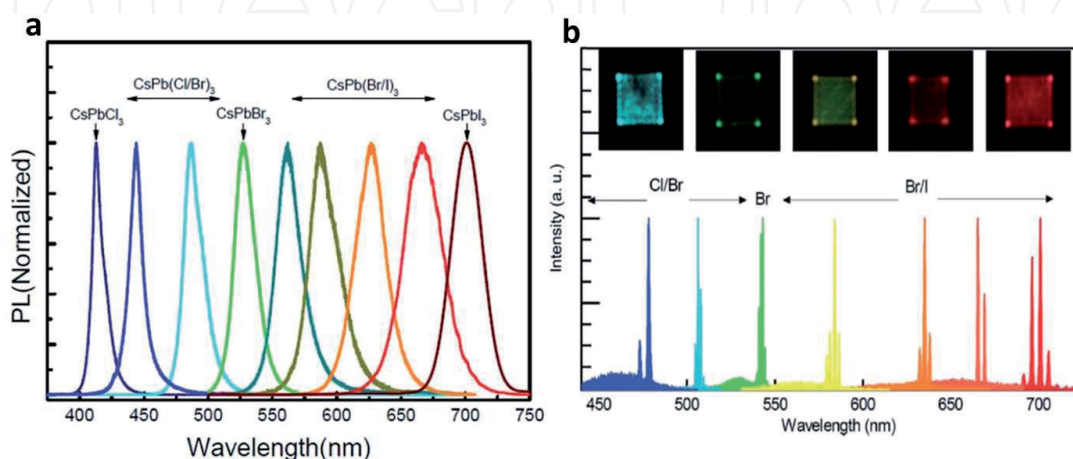


Figure 12.

(a) Photoluminescence spectra of $\text{CsPb}(X = \text{Cl, Br, I})_3$ nanoplatelets and (b) wavelength adjustment of perovskite lasing by controlling the content of halide in CsPbX_3 perovskite [6, 7, 57]. There is really an extraordinary point about nanowires is that they have very little carrier capture area and the laser quantum efficiency reaches to 100% (reproduced with permission of Ref. [6]).

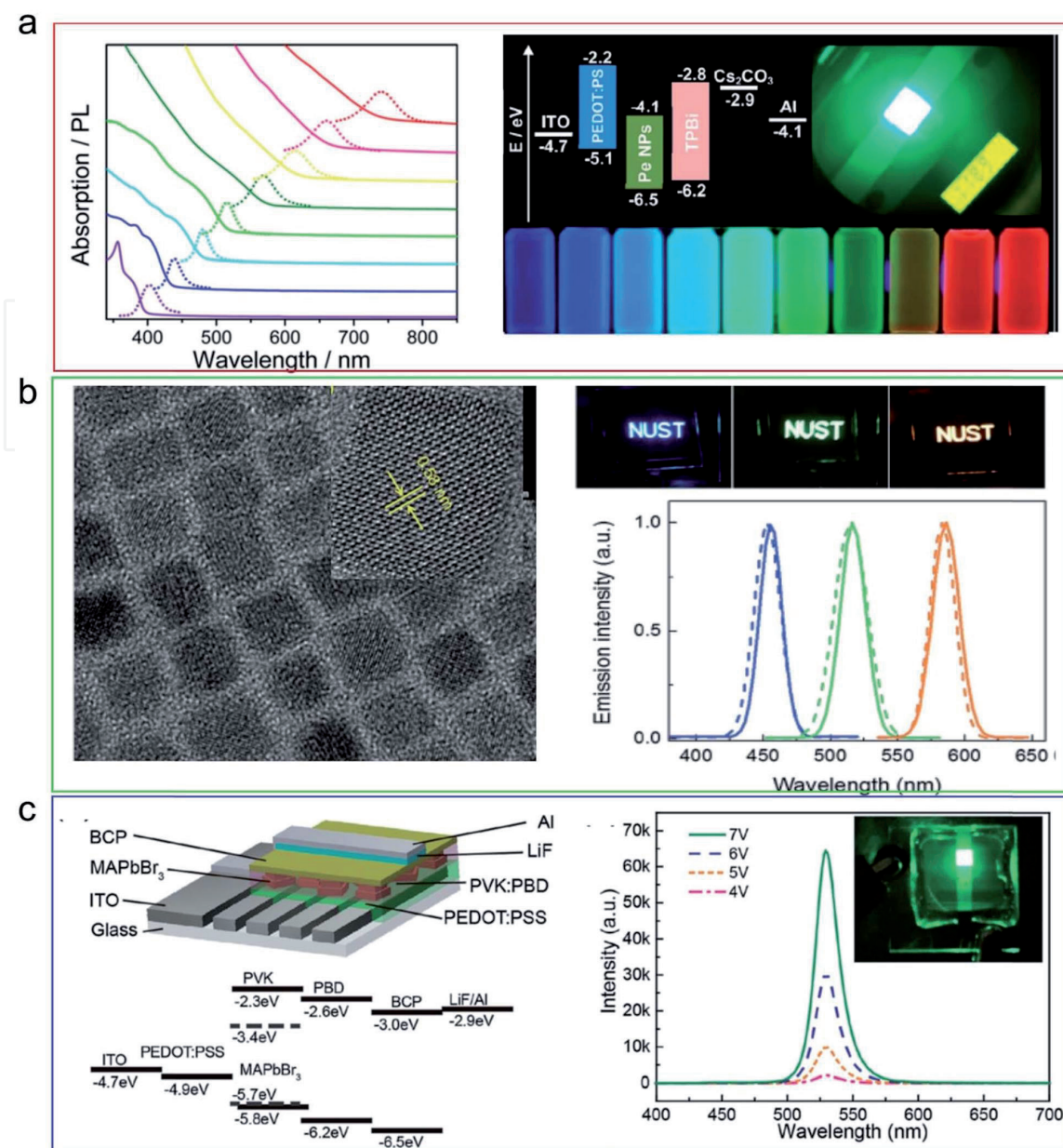


Figure 13.
In LED applications are generally used a low dimensional perovskite. (a) $\text{CH}_3\text{NH}_3\text{PbX}_3$ quantum dots are applied to fabricate LED, (b) CsPbX_3 quantum dots are used to form LED, (c) $\text{CH}_3\text{NH}_3\text{PbX}_3$ nanoplatelets are performed to obtain LED (reproduced with permission of Refs. [25, 89, 91]).

response time compared to the obtained photodetectors bulk perovskite and other inorganic nanowire photodetectors is higher in terms of response time of 0.3 ms, 1.3 A W^{-1} response and a detectivity of 2.5×10^{12} Jones. Park et al. show a remarkable perovskite nanomaterials application that Quantum dots were used as a single photon emitter at standard conditions. CsPbX_3 perovskite was used as the leading material to synthesize cubic shapes and quantum dots with an average size of 10 nm. Perovskite quantum dots displayed an excellent photon beam of emitted light and photoluminescence (PL) intensity fluctuations associated with PL life. It is defined that phenomenon as “A-type flashing” that is popular in the quantum dot system.

6. Conclusion

In this chapter, preparation methods and applications of 2D perovskite nanoparticles were reviewed. The most crucial points for synthesis method are uniformity

and form factor of synthesised nanoparticles. Furthermore, structural, optic, and electrochemical properties of 2D perovskites have been introduced in detail. Due to the low ionic interaction in the crystal structures, organo-halide perovskites exhibit low stability under ambient conditions. However, 2D perovskite nanoparticles still offer a great potential due to the structure-dependent optic and electronic properties.

Author details

Burak Gultekin^{1*}, Ali Kemal Havare², Shirin Siyahjani¹, Halil Ibrahim Ciftci³ and Mustafa Can⁴

¹ Ege University, Solar Energy Institute, Izmir, Turkey

² Faculty of Engineering, Electric and Electronics Engineering, Photoelectronic Lab. (PEL), Toros University, Mersin, Turkey

³ Faculty of Life Sciences, Medicinal and Biological Chemistry Science Farm Joint Research Laboratory, Kumamoto University, Kumamoto, Japan

⁴ Faculty of Engineering and Architecture, Izmir Katip Celebi University, Izmir, Turkey

*Address all correspondence to: burakgultekin@gmail.com

IntechOpen

© 2020 The Author(s). Licensee IntechOpen. This chapter is distributed under the terms of the Creative Commons Attribution License (<http://creativecommons.org/licenses/by/3.0>), which permits unrestricted use, distribution, and reproduction in any medium, provided the original work is properly cited. 

References

- [1] Tsai H et al. *High-efficiency two-dimensional Ruddlesden–Popper perovskite solar cells*. Nature. 2016;**536**(7616):312–316
- [2] Liu M, Johnston MB, Snaith HJ. *Efficient planar heterojunction perovskite solar cells by vapour deposition*. Nature. 2013;**501**(7467):395–398
- [3] Burschka J et al. *Sequential deposition as a route to high-performance perovskite-sensitized solar cells*. Nature. 2013;**499**(7458):316–319
- [4] Yuan M et al. *Perovskite energy funnels for efficient light-emitting diodes*. Nature nanotechnology. 2016;**11**(10):872–877
- [5] Tan Z-K et al. *Bright light-emitting diodes based on organometal halide perovskite*. Nature nanotechnology. 2014;**9**(9):687–692
- [6] Zhu H et al. *Lead halide perovskite nanowire lasers with low lasing thresholds and high quality factors*. Nature materials. 2015;**14**(6):636–642
- [7] Zhang Q et al. *Room-temperature near-infrared high-Q perovskite whispering-gallery planar nanolasers*. Nano letters. 2014;**14**(10):5995–6001
- [8] Miao J et al. *Highly Sensitive Organic Photodetectors with Tunable Spectral Response under Bi-Directional Bias*. Advanced Optical Materials. 2016;**4**(11):1711–1717
- [9] Miao J, Zhang F. *Recent progress on highly sensitive perovskite photodetectors*. Journal of Materials Chemistry C. 2019;**7**(7):1741–1791
- [10] Miao J et al. *Photomultiplication type organic photodetectors with broadband and narrowband response ability*. Advanced Optical Materials. 2018;**6**(8):1800001
- [11] Li L et al. *Achieving EQE of 16,700% in P3HT: PC 71 BM based photodetectors by trap-assisted photomultiplication*. Scientific reports. 2015;**5**(1):1–7
- [12] Li L et al. *Revealing the working mechanism of polymer photodetectors with ultra-high external quantum efficiency*. Physical Chemistry Chemical Physics. 2015;**17**(45):30712–30720
- [13] Jung S et al. *Enhancement of Photoluminescence Quantum Yield and Stability in CsPbBr₃ Perovskite Quantum Dots by Trivalent Doping*. Nanomaterials. 2020;**10**(4):710
- [14] Zhang D et al. *Increasing Photoluminescence Quantum Yield by Nanophotonic Design of Quantum-Confined Halide Perovskite Nanowire Arrays*. Nano letters. 2019;**19**(5):2850–2857
- [15] Khan Y et al. *Waterproof perovskites: high fluorescence quantum yield and stability from a methylammonium lead bromide/formate mixture in water*. Journal of Materials Chemistry C. 2020
- [16] Dong, Q., et al., *Operational stability of perovskite light emitting diodes*. Journal of Physics: Materials, 2020. **3**(1): p. 012002.
- [17] Stylianakis MM et al. *Inorganic and hybrid perovskite based laser devices: a review*. Materials. 2019;**12**(6):859
- [18] Schmidt LC et al. *Nontemplate synthesis of CH₃NH₃PbBr₃ perovskite nanoparticles*. Journal of the American Chemical Society. 2014;**136**(3):850–853
- [19] Chen D, Chen X. *Luminescent perovskite quantum dots: synthesis, microstructures, optical properties and applications*. Journal of Materials Chemistry C. 2019;**7**(6):1413–1446
- [20] Zhang C, Kuang DB, Wu WQ. *A Review of Diverse Halide Perovskite*

Morphologies for Efficient Optoelectronic Applications. Small Methods. 2020;**4**(2):1900662

[21] Ha S-T et al. *Metal halide perovskite nanomaterials: synthesis and applications*. Chemical science. 2017;**8**(4):2522-2536

[22] Gopinathan N et al. *Solvents driven structural, morphological, optical and dielectric properties of lead free perovskite CH₃NH₃SnCl₃ for optoelectronic applications: Experimental and DFT study*. Materials Research Express. 2020

[23] Shamsi J et al. *Metal halide perovskite nanocrystals: synthesis, post-synthesis modifications, and their optical properties*. Chemical reviews. 2019;**119**(5):3296-3348

[24] Shen D et al. *Understanding the solvent-assisted crystallization mechanism inherent in efficient organic-inorganic halide perovskite solar cells*. Journal of Materials Chemistry A. 2014;**2**(48):20454-20461

[25] Xing J et al. *High-efficiency light-emitting diodes of organometal halide perovskite amorphous nanoparticles*. ACS nano. 2016;**10**(7):6623-6630

[26] Zhang F et al. *Brightly luminescent and color-tunable colloidal CH₃NH₃PbX₃ (X= Br, I, Cl) quantum dots: potential alternatives for display technology*. ACS nano. 2015;**9**(4):4533-4542

[27] Pathak S et al. *Perovskite crystals for tunable white light emission*. Chemistry of Materials. 2015;**27**(23):8066-8075

[28] Tyagi P, Arveson SM, Tisdale WA. *Colloidal organohalide perovskite nanoplatelets exhibiting quantum confinement*. The journal of physical chemistry letters. 2015;**6**(10):1911-1916

[29] Hassan Y et al. *Structure-Tuned Lead Halide Perovskite Nanocrystals*. Advanced materials. 2016;**28**(3):566-573

[30] Luo B et al. *Synthesis, optical properties, and exciton dynamics of organolead bromide perovskite nanocrystals*. The Journal of Physical Chemistry C. 2015;**119**(47):26672-26682

[31] Wang Y et al. *Thermodynamically stabilized β -CsPbI₃-based perovskite solar cells with efficiencies > 18%*. Science. 2019;**365**(6453):591-595

[32] Shi J et al. *Efficient and stable CsPbI₃ perovskite quantum dots enabled by in situ ytterbium doping for photovoltaic applications*. Journal of Materials Chemistry A. 2019;**7**(36):20936-20944

[33] Wang A et al. *Controlled synthesis of lead-free and stable perovskite derivative Cs₂SnI₆ nanocrystals via a facile hot-injection process*. Chemistry of Materials. 2016;**28**(22):8132-8140

[34] Protesescu L et al. *Nanocrystals of cesium lead halide perovskites (CsPbX₃, X= Cl, Br, and I): novel optoelectronic materials showing bright emission with wide color gamut*. Nano letters. 2015;**15**(6):3692-3696

[35] Lim S-C et al. *Binary halide, ternary perovskite-like, and perovskite-derivative nanostructures: hot injection synthesis and optical and photocatalytic properties*. Nanoscale. 2017;**9**(11):3747-3751

[36] Shi, P., et al., *Template-Assisted Formation of High-Quality α -Phase HC (NH₂)₂PbI₃ Perovskite Solar Cells*. Advanced Science, 2019. **6**(21): p. 1901591.

[37] Ashley MJ et al. *Templated synthesis of uniform perovskite nanowire arrays*. Journal of the American Chemical Society. 2016;**138**(32):10096-10099

[38] Malgras V et al. *Hybrid methylammonium lead halide perovskite nanocrystals confined in gyroidal silica templates*. Chemical Communications. 2017;**53**(15):2359-2362

- [39] Ananthakumar S, Babu SM. *Progress on synthesis and applications of hybrid perovskite semiconductor nanomaterials—A review*. Synthetic Metals. 2018;**246**:64-95
- [40] Pileni M-P. *The role of soft colloidal templates in controlling the size and shape of inorganic nanocrystals*. Nature materials. 2003;**2**(3):145-150
- [41] Huang H et al. *Emulsion synthesis of size-tunable CH₃NH₃PbBr₃ quantum dots: an alternative route toward efficient light-emitting diodes*. ACS applied materials & interfaces. 2015;**7**(51):28128-28133
- [42] Wali Q et al. *Advances in stability of perovskite solar cells*. Organic Electronics. 2020;**78**:105590
- [43] Wang, R., et al., *A review of perovskites solar cell stability*. Advanced Functional Materials, 2019. **29**(47): p. 1808843.
- [44] Heo JH et al. *Efficient inorganic-organic hybrid heterojunction solar cells containing perovskite compound and polymeric hole conductors*. Nature photonics. 2013;**7**(6):486
- [45] Etgar L. *The merit of perovskite's dimensionality; can this replace the 3D halide perovskite?* Energy & Environmental Science. 2018;**11**(2):234-242
- [46] Ma C et al. *High performance low-dimensional perovskite solar cells based on a one dimensional lead iodide perovskite*. Journal of Materials Chemistry A. 2019;**7**(15):8811-8817
- [47] Zhu P, Zhu J. *Low-dimensional metal halide perovskites and related optoelectronic applications*. InfoMat. 2020;**2**(2):341-378
- [48] Kulkarni SA et al. *Perovskite Nanoparticles: Synthesis, Properties, and Novel Applications in Photovoltaics and LEDs*. Small Methods. 2019;**3**(1):1800231
- [49] Sichert JA et al. *Quantum size effect in organometal halide perovskite nanoplatelets*. Nano letters. 2015;**15**(10):6521-6527
- [50] Wang J et al. *Interfacial control toward efficient and low-voltage perovskite light-emitting diodes*. Advanced Materials. 2015;**27**(14):2311-2316
- [51] Hong WL et al. *Efficient low-temperature solution-processed lead-free perovskite infrared light-emitting diodes*. Advanced Materials. 2016;**28**(36):8029-8036
- [52] Bade SGR et al. *Fully printed halide perovskite light-emitting diodes with silver nanowire electrodes*. ACS nano. 2016;**10**(2):1795-1801
- [53] Li G et al. *Highly efficient perovskite nanocrystal light-emitting diodes enabled by a universal crosslinking method*. Advanced Materials. 2016;**28**(18):3528-3534
- [54] Veldhuis SA et al. *Perovskite materials for light-emitting diodes and lasers*. Advanced Materials. 2016;**28**(32):6804-6834
- [55] Liang D et al. *Color-pure violet-light-emitting diodes based on layered lead halide perovskite nanoplates*. ACS nano. 2016;**10**(7):6897-6904
- [56] Yantara N et al. *Inorganic halide perovskites for efficient light-emitting diodes*. The journal of physical chemistry letters. 2015;**6**(21):4360-4364
- [57] Zhang Q et al. *High-quality whispering-gallery-mode lasing from cesium lead halide perovskite nanoplatelets*. Advanced Functional Materials. 2016;**26**(34):6238-6245

- [58] Fu Y et al. *Nanowire lasers of formamidinium lead halide perovskites and their stabilized alloys with improved stability*. Nano letters. 2016;**16**(2):1000-1008
- [59] Nedelcu G et al. *Fast anion-exchange in highly luminescent nanocrystals of cesium lead halide perovskites (CsPbX₃, X= Cl, Br, I)*. Nano letters. 2015;**15**(8):5635-5640
- [60] Akkerman QA et al. *Tuning the optical properties of cesium lead halide perovskite nanocrystals by anion exchange reactions*. Journal of the American Chemical Society. 2015;**137**(32):10276-10281
- [61] Wu K et al. *Ultrafast interfacial electron and hole transfer from CsPbBr₃ perovskite quantum dots*. Journal of the American Chemical Society. 2015;**137**(40):12792-12795
- [62] Huang H et al. *Colloidal lead halide perovskite nanocrystals: synthesis, optical properties and applications*. NPG Asia Materials. 2016;**8**(11):e328-e328
- [63] Noh JH et al. *Chemical management for colorful, efficient, and stable inorganic-organic hybrid nanostructured solar cells*. Nano letters. 2013;**13**(4):1764-1769
- [64] Tanaka K et al. *Comparative study on the excitons in lead-halide-based perovskite-type crystals CH₃NH₃PbBr₃ CH₃NH₃PbI₃*. Solid state communications. 2003;**127**(9-10):619-623
- [65] Umebayashi T et al. *Electronic structures of lead iodide based low-dimensional crystals*. Physical Review B. 2003;**67**(15):155405
- [66] Schulz P et al. *Interface energetics in organo-metal halide perovskite-based photovoltaic cells*. Energy & Environmental Science. 2014;**7**(4):1377-1381
- [67] Eperon GE et al. *Formamidinium lead trihalide: a broadly tunable perovskite for efficient planar heterojunction solar cells*. Energy & Environmental Science. 2014;**7**(3):982-988
- [68] Protesescu L et al. *Monodisperse formamidinium lead bromide nanocrystals with bright and stable green photoluminescence*. Journal of the American Chemical Society. 2016;**138**(43):14202-14205
- [69] Lignos I et al. *Unveiling the shape evolution and halide-ion-segregation in blue-emitting formamidinium lead halide perovskite nanocrystals using an automated microfluidic platform*. Nano letters. 2018;**18**(2):1246-1252
- [70] Minh DN et al. *Room-temperature synthesis of widely tunable formamidinium lead halide perovskite nanocrystals*. Chemistry of Materials. 2017;**29**(13):5713-5719
- [71] Hao F et al. *Lead-free solid-state organic-inorganic halide perovskite solar cells*. Nature photonics. 2014;**8**(6):489
- [72] Jellicoe TC et al. *Synthesis and optical properties of lead-free cesium tin halide perovskite nanocrystals*. Journal of the American Chemical Society. 2016;**138**(9):2941-2944
- [73] Chen Q et al. *Under the spotlight: The organic-inorganic hybrid halide perovskite for optoelectronic applications*. Nano Today. 2015;**10**(3):355-396
- [74] Zhang D et al. *Synthesis of composition tunable and highly luminescent cesium lead halide nanowires through anion-exchange reactions*. Journal of the American Chemical Society. 2016;**138**(23):7236-7239
- [75] Tong Y et al. *From precursor powders to CsPbX₃ perovskite nanowires: one-pot synthesis, growth mechanism, and oriented self-assembly*. Angewandte

Chemie International Edition.
2017;**56**(44):13887-13892

[76] Brennan MC et al. *Origin of the size-dependent stokes shift in CsPbBr₃ perovskite nanocrystals*. Journal of the American Chemical Society. 2017;**139**(35):12201-12208

[77] Brennan MC, Zinna J, Kuno M. *Existence of a size-dependent Stokes shift in CsPbBr₃ perovskite nanocrystals*. ACS Energy Letters. 2017;**2**(7):1487-1488

[78] Huang G et al. *Postsynthetic Doping of MnCl₂ Molecules into Preformed CsPbBr₃ Perovskite Nanocrystals via a Halide Exchange-Driven Cation Exchange*. Advanced materials. 2017;**29**(29):1700095

[79] Gonzalez-Carrero S et al. *The luminescence of CH₃NH₃PbBr₃ perovskite nanoparticles crests the summit and their photostability under wet conditions is enhanced*. Small. 2016;**12**(38):5245-5250

[80] Liu F et al. *Highly luminescent phase-stable CsPbI₃ perovskite quantum dots achieving near 100% absolute photoluminescence quantum yield*. ACS nano. 2017;**11**(10):10373-10383

[81] Tong Y et al. *Highly luminescent cesium lead halide perovskite nanocrystals with tunable composition and thickness by ultrasonication*. Angewandte Chemie International Edition. 2016;**55**(44):13887-13892

[82] Koscher BA et al. *Essentially trap-free CsPbBr₃ colloidal nanocrystals by postsynthetic thiocyanate surface treatment*. Journal of the American Chemical Society. 2017;**139**(19):6566-6569

[83] Meinardi F et al. *Doped halide perovskite nanocrystals for reabsorption-free luminescent solar concentrators*. ACS Energy Letters. 2017;**2**(10):2368-2377

[84] Giansante C, Infante I. *Surface traps in colloidal quantum dots: a combined experimental and theoretical perspective*. The journal of physical chemistry letters. 2017;**8**(20):5209-5215

[85] He M et al. *Mn-Doped cesium lead halide perovskite nanocrystals with dual-color emission for WLED*. Dyes and Pigments. 2018;**152**:146-154

[86] Liu M et al. *Aluminum-Doped Cesium Lead Bromide Perovskite Nanocrystals with Stable Blue Photoluminescence Used for Display Backlight*. Advanced Science. 2017;**4**(11):1700335

[87] Pan G et al. *Doping lanthanide into perovskite nanocrystals: highly improved and expanded optical properties*. Nano letters. 2017;**17**(12):8005-8011

[88] Xing J et al. *Vapor phase synthesis of organometal halide perovskite nanowires for tunable room-temperature nanolasers*. Nano letters. 2015;**15**(7):4571-4577

[89] Song J et al. *Quantum dot light-emitting diodes based on inorganic perovskite cesium lead halides (CsPbX₃)*. Advanced materials. 2015;**27**(44):7162-7167

[90] Liu J et al. *Two-dimensional CH₃NH₃PbI₃ perovskite: Synthesis and optoelectronic application*. ACS nano. 2016;**10**(3):3536-3542

[91] Ling Y et al. *Bright light-emitting diodes based on organometal halide perovskite nanoplatelets*. Advanced materials. 2016;**28**(2):305-311